

# OPTIMAL DESIGN OF WHEEL PROFILE FOR RAILWAY VEHICLES

I.Y. Shevtsov, V.L. Markine, C. Esveld  
Section of Road and Railway Engineering  
Faculty of Civil Engineering and Geosciences, Delft University of Technology  
Stevinweg 1, NL-2628, CN Delft,  
The Netherlands

I.Y.Shevtsov@CiTG.TUdelft.NL, V.L.Markine@CiTG.TUdelft.NL, C.Esveld@CiTG.TUdelft.NL  
<http://www.rail.tudelft.nl/>

## Abstract

Beyond the advantages in design of running gear and railway vehicles itself and introducing the active wheelset steering control systems many railroads and tram companies still use huge number of old fashion vehicles. Dynamic performance, safety and maintenance cost of which strongly depend on the wheelset dynamics and particularly on how good is design of wheel and rail profiles. The paper presents a procedure for design of a wheel profile based on geometrical wheel/rail (w/r) contact characteristics which uses numerical optimization technique. The procedure has been developed by Railway Engineering Group in Delft University of Technology. The optimality criteria formulated using the requirements to railway track and wheelset, are related to stability of wheelset, cost efficiency of design and minimum wear of wheels and rails. The shape of a wheel profile has been varied during optimization. A new wheel profile is obtained for given target rolling radii difference function '  $y - \Delta r$  ' and rail profile. Measurements of new and worn wheel and rail profiles has been used to define the target '  $y - \Delta r$  ' curve. Finally dynamic simulations of vehicle with obtained wheel profile have been performed in ADAMS/Rail program package in order to control w/r wear and safety requirements. The proposed procedure has been applied to design of wheel profile for trams. Numerical results are presented and discussed.

*Keywords:* Profile design, Optimization, Geometrical contact, Tram

## 1. Introduction

Huge progress has been made in design of running gears and railway vehicles. Tilting trains, high speed trains, active steering wheelset and many other brilliant solutions had been implemented in recent years on the railways. But beyond this progress the mechanics of railway wheelset remains the same and an inappropriate combination of wheel and rail profiles can vanish all this technological advances. And also a lot of old fashion vehicles are still in good condition to be replaced but they especially need appropriate combination of wheel/rail profiles, because they do not have high-tech devices which improving performance.

Problem of wheel/rail profiles design exists for many years and different approaches have been developed to obtain satisfactory wheel/rail profile combinations. It is possible to find an optimal combination of wheel and rail profile when dealing with closed railway system, i.e. when the same type of rolling stock is running on the same track and no influence of other type railway vehicles presents. Example of such systems includes heavy haul and tramlines. Due to the fact that a rail costs much more than a wheel and wheels are more often re-profiled, it looks attractive to design a new wheel profile, which matches an existing rail profile.

Using geometrical characteristics of a contact between wheel and rail it is possible to judge about dynamic parameters of wheelset and ultimately parameters of vehicle since a wheelset represents a source of disturbances from track to vehicle. The wheel-rail geometry plays a dominant role in vehicle lateral dynamics. When a wheelset travels along a track the centre of axle makes the sinusoidal movement. The rolling radii, contact angles and the wheelset roll angle vary as the wheelset moves laterally relative to the rails. The nature of the functional dependence between these geometrically constrained variables and the wheelset lateral position depends on the wheel and rail cross-sectional shape. One of important characteristics of the wheel-rail contact is the rolling radius of a wheel at the contact point [1], which is in fact different for the right and left wheel ( $r_1$  and  $r_2$  respectively in Fig. 1). When a wheelset is in a central position the rolling radii of both wheels are the same, i.e.  $r_1 = r_2 = r$ . An instantaneous difference between rolling radii

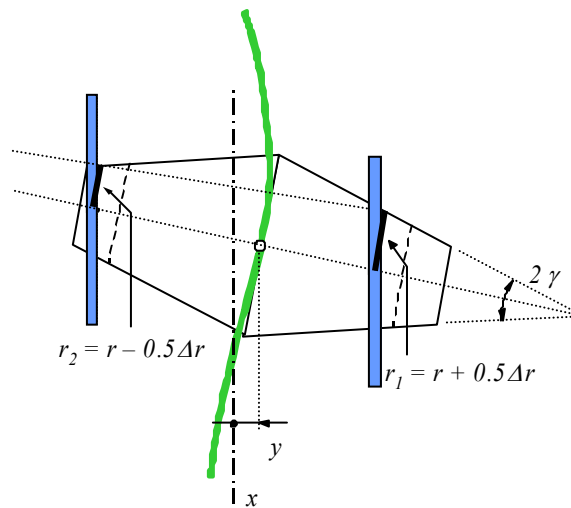


Fig. 1. Rolling radii ( $r_1$  and  $r_2$ ) corresponding to wheelset displacement  $y$

of the right and left wheels  $\Delta r \equiv r_1 - r_2$  is defined as a function of the lateral displacement  $y$  of the wheelset with respect to the central position. An example of a rolling radii difference for conical and worn profiles (also known as a ‘ $y - \Delta r$ ’ curve) is shown in Fig. 2. Generally, it is a non-linear function of the lateral displacement  $y$  of a wheelset. Due to the wear of wheels the wheel profile is changing and consequently  $\Delta r$  is changing as shown in Fig. 2. It is known, for example, that the rolling radii difference often changes faster with wheelset lateral position for hollow contour worn wheels than for new 1/20 taper wheels (in other words, the conicity is usually larger for worn wheels).

The rolling radii enter the wheelset equations of motion due to the difference between the rolling radii of the two wheels of the wheelset. A rolling radii difference is one of the main characteristics that describes a contact between wheelset and railway track, which in turn defines the dynamic behaviour of a wheelset [1, 2].

Determination of geometric contact characteristics for given wheel and rail profiles, wheel and rail gauge, and railhead cant angles is a well-known and solved problem for many years. These nonlinearities have been investigated by Wickens [3], Cooperrider [4], and De Pater [5]. The linear conical wheel profile widely used before has burst linear characteristics of rolling radii difference (see Fig. 2), that results in shocks during a contact between wheel flange and rail at a motion of wheelset. The worn wheel usually has the smooth continuous characteristics of a contact. However high conicity of a worn wheel reduces critical speed of a wheelset and results in high oscillations of vehicle. Naturally, there is a desire to find a compromise between these two extremes. A traditional way to achieve the compromise is by trying different wheel profiles, with the purpose to find one of it with the characteristics satisfied to given conditions (usually curving, hunting, and contact stresses are taken into account).

However, this is very time consuming and extremely ineffective way. More attractive way is a numerical solution of an inverse problem, i.e. design of a wheel profile based on a given rolling radii difference  $\Delta r$  and rail profile. If a

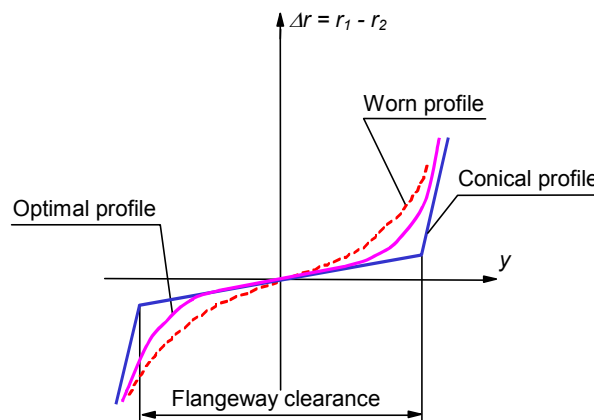


Fig. 2. Rolling radii difference vs. lateral displacement of wheelset curve (‘ $y - \Delta r$ ’ curve)

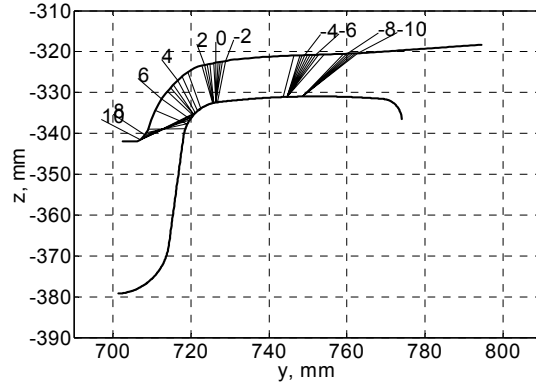


Fig. 3. Wheel and rail contact

function of rolling radii difference from the lateral displacement of wheelset and the rail profile are known one can try to find a corresponding profile of a wheel. However, there is no direct way of the solution of this problem. Here, the problem of determination of wheel profile for given ‘ $y - \Delta r$ ’ curve and rail profile has been formulated as an optimization problem. The problem and numerical method used to solve it are described below.

## 2. Design procedure

The procedure of wheel profile design consists of several steps. It starts from the definition of the target ‘ $y - \Delta r$ ’ function. For this wheel and rail profile measurements can be used. During this stage data about new and worn profiles have been collected. The next step is to process these measurements and obtain data, which will be used during the design of wheel. The ‘ $y - \Delta r$ ’ curves for different wheel/rail combinations have been analysed and target ‘ $y - \Delta r$ ’ function have been obtained. After this stage the optimization problem has to be formulated and solved which results in a new wheel profile. The obtained profile should be controlled on dynamic performance, satisfaction to the wear and safety requirements. Here, vehicle dynamic simulations have been performed using ADAMS/Rail software. If the tests are failed the optimization procedure has to be repeated with new target ‘ $y - \Delta r$ ’ and the dynamic tests has to be performed again. Otherwise the obtained wheel profile is taken as optimum one.

The contact situations between right wheel and rail for different lateral displacement of wheelset are shown on Fig. 3. The wheel and rail profiles are unworn. Lines between wheel and rail profiles connect corresponding contact points and values of corresponding lateral displacements are shown above wheel profile. It is easy to see that for zero lateral displacement contact points locates near the flange root and gauge corner of rail. After a small (2 mm) lateral displacement contact point jumps along the profile and this lead to gap in rolling radii and reduce dynamic performance. For optimized profile such jumps should be reduced which means that the corresponding rolling radii function has to be continuous.

A target rolling radii difference function can be obtained in several ways.

- It can be modified rolling radii difference function for an existing wheel profile.
- It is also possible to use the average ‘ $y - \Delta r$ ’ curve for the worn wheels as a target function.

The target ‘ $y - \Delta r$ ’ curve can be built based on designer experience as well.

All these concepts will be discussed in details in the consequent sections.

## 3. Formulation of optimization problem

To make use of numerical optimization techniques an optimization problem should be stated in a general form that reads:

Minimize

$$F_0(\mathbf{x}) \rightarrow \min, \quad \mathbf{x} \in R^N \quad (1)$$

subject to

$$F_j(\mathbf{x}) \leq 1, \quad j = 1, \dots, M \quad (2)$$

and

$$A_i \leq x_i \leq B_i, \quad i = 1, \dots, N \quad (3)$$

where

$F_0$  is the objective function ;

$F_j, \quad j = 1, \dots, M$  are the constrains

$\mathbf{x} = [x_1, \dots, x_N]^T$  is the vector of design variables;

$A_i$  and  $B_i$  are the side limits, which define lower and upper bounds of the  $i$ -th design variable.

Components of the vector  $x$  represent various parameters of a structure, such as geometry, material, stiffness and damping properties, which can be varied to improve the design performance. Depending on the problem under consideration the objective and constraint functions (1)-(2) can describe various structural and dynamic response quantities such as weight, reaction forces, stresses, natural frequencies, displacements, velocities, accelerations, etc. Cost, maintenance and safety requirements can be used in the formulation of the optimization problem as well. The objective function provides a basis for improvement of the design whereas the constraints impose some limitations on behavior characteristics of a structure.

Formulated in the form (1)-(3) the optimization problem can be solved using one of the conventional methods of Nonlinear Mathematical Programming (NMP).

### 3.1. Design variables

Positions of several points on the flange, flange root and wheel tread have been taken as design variables. Connected by piecewise cubic Hermite interpolating polynomial these points define the wheel profile (Fig. 4). To limit a search region and exclude unrealistic profiles, constraints on the shape of a wheel profile have been introduced. Positions of the design variables have been fixed along horizontal axis but could be moved in vertical direction. Points on flange top and conical part of profile have been fixed (Fig. 4). During initial computations the number of design variables and their positions along the  $y$  axes have been determined. Starting from 5 design variables and then increasing their number up to 10 design variables, finally 14 design variables have been chosen which are situated along the wheel flange, flange root and tread, i.e.

$$\mathbf{x} = [y_1, \dots, y_{14}], \quad (4)$$

where  $y_i$  are the vertical coordinates of varied points. The design variables are shown on Fig. 4.

### 3.2. Objective function

The requirement reflecting the minimum discrepancy between the target rolling radii difference function and the one for design profile can be written as:

$$F_0(\mathbf{x}) \equiv \frac{\sum_{i=1}^K (\Delta r_{yi}^{tar}(\mathbf{x}) - \Delta r_{yi}^{calc}(\mathbf{x}))^2}{\sum_{i=1}^K (\Delta r_{yi}^{tar}(\mathbf{x}))^2} \rightarrow \min, \quad (5)$$

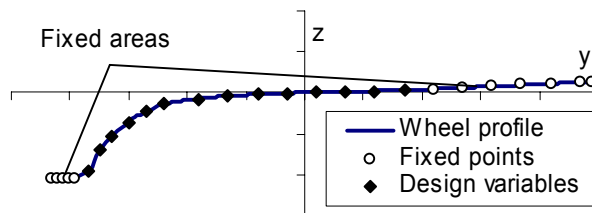


Fig. 4. Wheel profile design variables and fixed points

where

$F_0(\mathbf{x})$  is the objective function;

$\Delta r_{yi}^{tar}(\mathbf{x})$  is the target rolling radii difference function;

$\Delta r_{yi}^{calc}(\mathbf{x})$  is the calculated rolling radii difference function for the design profile.

The function (5) has been taken as the objective function of the optimization problem (1) - (3). Some of the requirements to optimized profile have been considered as constrains (5). They are discussed below.

### 3.3. Stability requirements

Equivalent (or effective) conicity  $\gamma_e$  [1, 2] is usually taken as wheelset stability parameter. For different types of railway vehicles the wheels with different equivalent conicity should be used to have required critical speed. High conicity can result in dynamic instability or “hunting”, which severely degrades the ride and can damage the track. The equivalent conicity range  $\gamma_e^{\max}$  for a wheel was set to avoid obtaining too high conicity of a new wheel:

$$F_1 \equiv (\gamma_e^{\max} - \gamma_e) / \gamma_e^{\max} \geq 0. \quad (6)$$

### 3.4. Safety requirements

Two safety requirements have been included. The first one is the requirement for wheel flange thickness, which is checked after the optimization. The second one is the requirement to avoid derailment of the vehicle which is achieved by restriction of minimal flange angle. This requirement has been checked only for the optimized profile.

### 3.5. Design requirements

Constrains on angles between neighbouring parts of profile were introduced to avoid hollow or convex parts on profile and therefore to exclude unrealistic wheel design during optimization. Design variables have been numbered from 1 to 14, starting from the low left side to the upper right of profile (see Fig. 4). Constrains for point number  $i$  have been written in following form:

$$F_j \equiv 1 - \frac{\gamma_{i+1}}{\gamma_i} \geq 0, \quad j = 2, \dots, 8, \quad i = 4, \dots, 10, \quad (7)$$

for the concave part of the profile and for the convex part of the profile:

$$F_j \equiv 1 - \frac{\gamma_i}{\gamma_{i+1}} \geq 0, \quad j = 9, \dots, 12, \quad i = 11, \dots, 14. \quad (8)$$

The  $\gamma_i$  is the angle between the axis  $y$  and the straight line connecting point  $i$  with point  $i+1$  of wheel profile and the  $\gamma_{i+1}$  is the angle between the axis  $y$  and the straight line connecting point  $i+1$  with point  $i+2$  of wheel profile.

The 11 design variables are checked and three first design variables situated on the flange are not checked, because they already constrained by bounds used in optimization problem.

## 4. Optimization method

The problem (4) – (8) has been solved using the MARS method (Multipoint Approximation based on Response Surface fitting) [6, 7]. The method has been specifically developed for problems where multiple response analyses and (time consuming) simulations are involved.

The MARS method is based on the approximation concepts [7, 8, 9] according to which the original minimization problem is replaced with a succession of simpler ones formulated for approximations of the original objective and

constraint functions. According to the MARS method, each approximation is defined as a function of the design variables  $\mathbf{x}$  and tuning parameters  $\mathbf{a}$ . To determine the components of vector  $\mathbf{a}$  the following weighted least-squares minimization problem is to be solved:

Find vector  $\mathbf{a}$  that minimizes

$$G(\mathbf{a}) = \sum_{p=1}^P \{w_p [F(\mathbf{x}_p) - \tilde{F}(\mathbf{x}_p, \mathbf{a})]^2\}. \quad (9)$$

Here  $F(\mathbf{x}_p)$  is the value of the original function evaluated at the point of the design parameter space  $\mathbf{x}_p$ , and  $P$  is the total number of such plan points;  $w_p$  is a weight factor that characterizes the relative contribution of the information about the original function at the point  $\mathbf{x}_p$ . The main issues of the MARS method such as building of approximation functions, planning of numerical experiments and move limit strategy are of scope of the paper. More information about the weight coefficient assignment, the move limits strategy and the most recent developments in the MARS method can be found in [6, 7, 10].

## 5. Dynamic check

When the optimization problem has been solved, the dynamic performance of the vehicle with the obtained wheel profile has to be checked. The tramcar was modelled in the ADAMS/Rail computational package. Standard ADAMS/Rail function have been used for calculation of the wear index. The wear index is calculated as follows (taken from the English Normatives (British Rail)).

$$W = F_1 \cdot \xi + F_2 \cdot \eta, \quad (10)$$

where:

$F_1$  - longitudinal creep force,

$\xi$  - longitudinal creepage,

$F_2$  - lateral creep force,

$\eta$  - lateral creepage (also see [11]).

In all presented cases the tram simulations has been performed for the 50m straight track with 40m transition curve switching into the 50 m right hand side curve with R=150m and than 30 m transition curve switching to the 230m tangent track. The vehicle travels with the speed 10m/s.

The wear index on the left wheel of first wheelset and lateral displacement of first wheelset has been chosen as the most representative quantities in the dynamic check. Based on lateral displacement of wheelset one can judge about stability of wheelset.

## 6. Numerical Results and Discussion

The computer package for design of wheel profiles for given rolling radii difference function (DoP) has been made. The design procedure was applied to design tram wheel profile. For our calculations the Ri60 rail profile with inclination 1:40 have been chosen and wheel profile HTM-2002 (used by HTM (The Hague tram company)) have been chosen as a starting (Initial) profile. The track has normal 1435 mm wide gauge.

After initial computations of geometric contact characteristics, it has been found that the wheelset inner gauge was too wide (originally it is 1389 mm with 530 mm distance between mean wheel circle and inside wheel side). It resulted in situations when even without lateral displacement the contact points were located on the gage corner of the rails and flange root of the wheels. After discussion with HTM the wheelset inner gauge was reduced by 4 mm and became 1385 mm.

Here the two examples of target function have been considered. In first case the mean ' $y - \Delta r$ ' curve (calculated for the set of ' $y - \Delta r$ ' curves for measured w/r profiles) have been used as target function. In second case the target function have been design on the base of ' $y - \Delta r$ ' function for non-worn profiles and mean ' $y - \Delta r$ ' function. The case when target function is made based on designer experience is described in [12].

## 6.1. Mean rolling radii difference

As initial step in design of new wheel the idea that the worn profiles usually have less wear because they better match rail profile was used. The set of rail profiles measured for straight and curved parts along the tramlines during a year period representing different stages of track wear has been used. Tram wheels also had been measured and collected into database representing set of different vehicles and different mileage. From this database the set of 18 rail profiles and 32 wheels with different mileage have been analysed. For all each combination of wheel and rail the corresponding ' $y - \Delta r$ ' curve has been calculated. After this the mean values of rolling radii difference were calculated for each step of lateral displacement of wheelset and the mean ' $y - \Delta r$ ' curve was obtained (Fig. 5). The grey round points on this figure represents calculated rolling radii differences and the black line corresponds to the mean ' $y - \Delta r$ ' curve. The values with opposite sign of rolling radii were obtained during the computations. The ' $y - \Delta r$ ' curve for Ri60 and HTM2002 w/r profiles (Initial) and the mean curve (Target\_mean) are presented on Fig. 6. The line with square marks corresponds to the computed curve for Initial profile, and the solid line with x marks shows the Target\_mean ' $y - \Delta r$ ' curve. Comparing these two functions one can see that mean curve has higher tangent. The wheel profile which has the closes rolling radii difference function to the mean ' $y - \Delta r$ ' curve has been obtained using the proposed method. Corresponding ' $y - \Delta r$ ' function (Optimized\_mean) is shown on Fig. 6 by line with empty rhombus marks. On Fig. 7 the Initial and Optimized\_mean wheel profiles are presented. The Optimized\_mean profiles has larger flange angle than Initial profile.

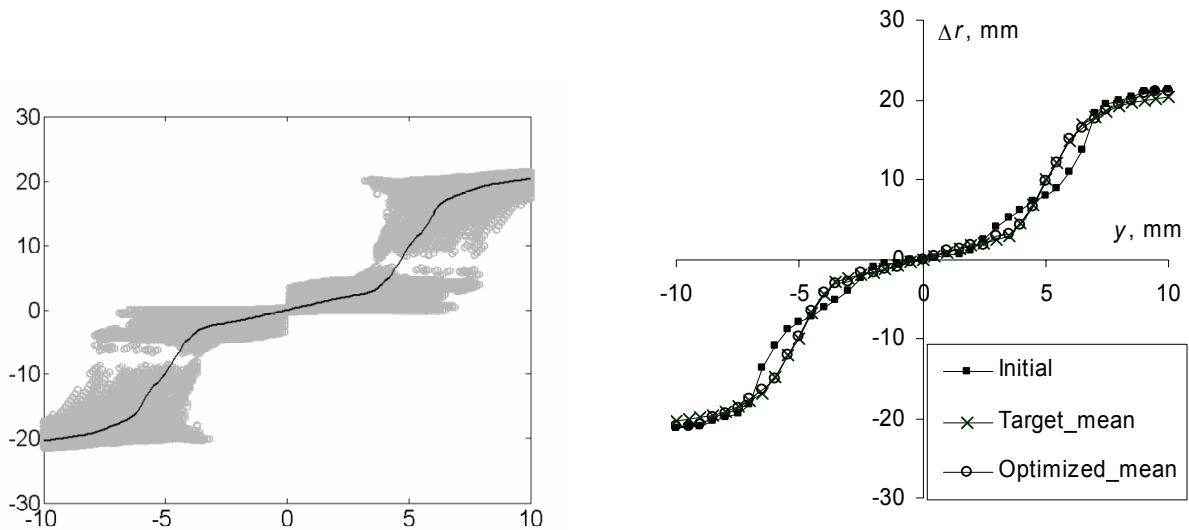


Fig. 5 Rolling radii difference for measured wheel and rail profiles and mean ' $y - \Delta r$ ' curve

Fig. 6. Rolling radii difference vs. lateral displacement of wheelset (Case - mean)

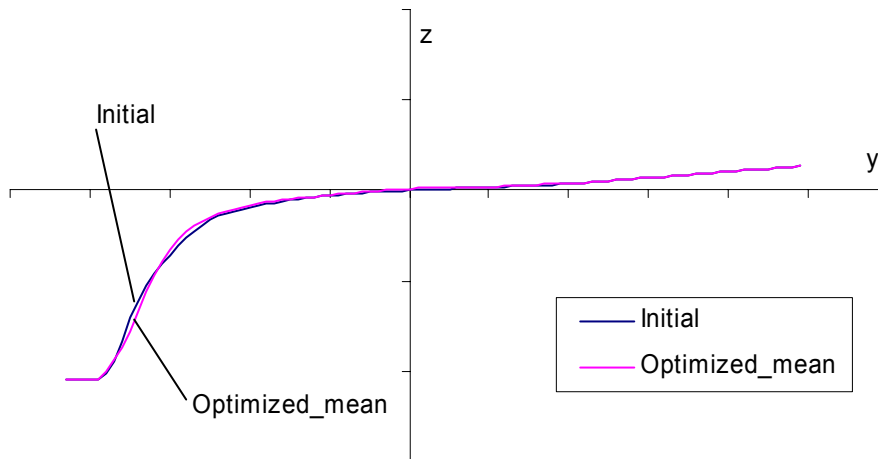


Fig. 7. Initial and Optimized\_mean wheel profiles (Case - mean)

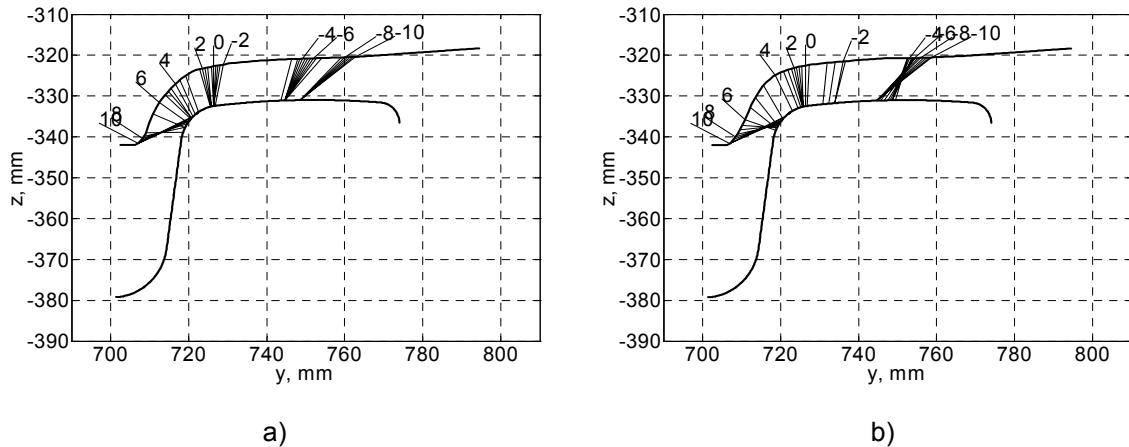


Fig. 8. Position of contact points on wheel and rail depending on lateral displacement of wheelset (Case - mean)

On Fig. 8 the Initial (a) and Optimized\_mean (b) wheel profiles contacting with Ri60 rail are shown. The contact points on the Optimized\_mean wheel are more evenly spread on the tread than on the Initial. The jump of contact point for 1 mm of lateral displacement and larger distances between contact points on flange result in instable behaviour of wheelset as it was confirmed by dynamic analysis.

On Fig. 9 and Fig. 10 results of dynamic simulation of a tramcar on Initial and Optimized\_mean wheels are presented. On Fig. 9 the lateral displacement of the first wheelset is shown. The wear index for left wheel is shown on Fig. 10. From these two figures one can clearly see that vehicle on Optimized\_mean wheels is unstable and has higher amount of wear in curve and especially on the tangent track. This can be explained by the fact that the conicity of Optimized\_mean wheel is very high – 0.47. Such conicity should definitely result in wheelset instability on straight track and high amount of wear. After the dynamic analysis of the results the second approach for creation of target curve has been chosen. According to it the target ‘ $y - \Delta r$ ’ has been obtained by modifying Initial and Target\_mean curves.

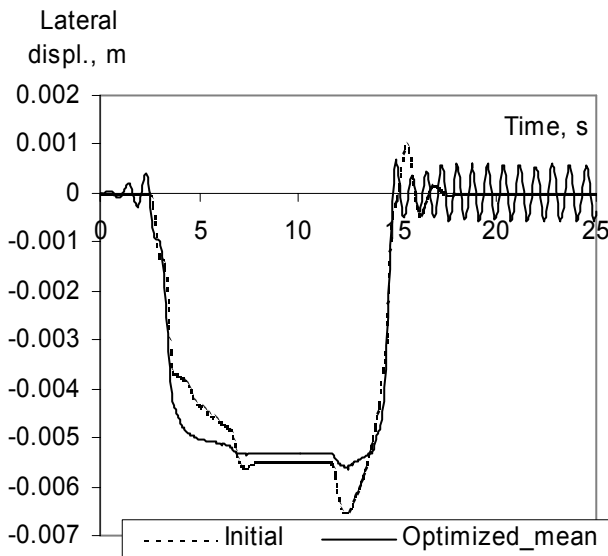


Fig 9. Lateral displacements of front wheelset vs. time (Case - mean)

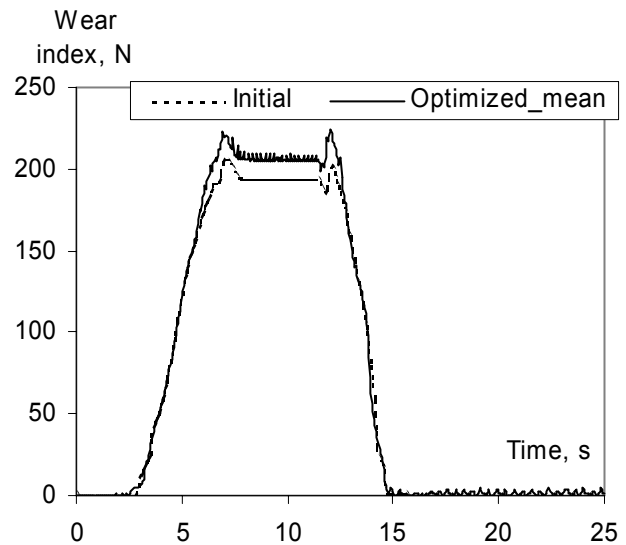


Fig 10. Wear index of the left front wheel vs. time (Case - mean)

## 6.2. Modified rolling radii difference

Based on Initial and Target\_mean a smooth target ‘ $y - \Delta r$ ’ curve has been created, which is shown on Fig. 11 (line with cross marks). The line with square marks corresponds to the computed curve for Initial profile, and the solid line with empty triangle marks shows the ‘ $y - \Delta r$ ’ curve for Optimized profile. The strategy of creation a target

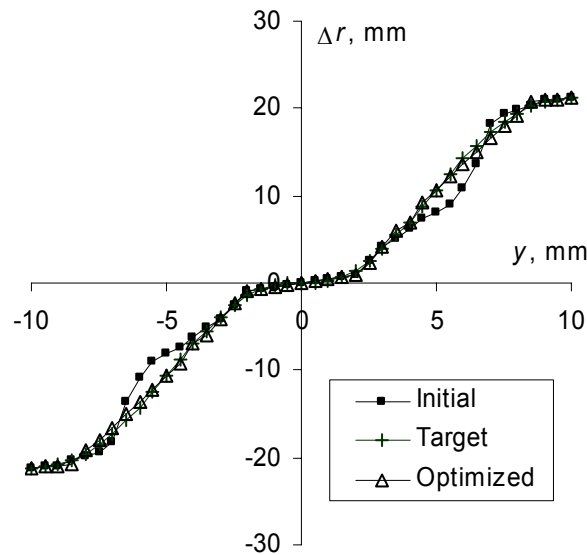


Fig. 11. Rolling radii difference vs. lateral displacement of wheelset (Case - design)

' $y - \Delta r$ ' curve was:

- to have small rolling radii difference for small lateral displacements of the wheelset, which gives us stability on the straight track
- to have higher rolling radii difference for big lateral displacements to have better curving and less wear.

On Fig. 12 the Initial and Optimized wheel profiles are shown. From comparison of the curves on Fig. 11 and Fig. 12 it can be easily seen that the rolling radii difference for Optimized profile is larger than the rolling radii difference for Initial profile in case of flange contact. Correspondingly, the wheel flange of Optimized wheel is arranged below the initial wheel profile.

Even though the Initial and Optimized wheel profiles are close to each other (Fig. 12) the corresponding ' $y - \Delta r$ ' curves are different (Fig. 11). The ' $y - \Delta r$ ' curve corresponding to the Optimized wheel profile is closer to the target ' $y - \Delta r$ ' curve, than the one corresponding to the initial design.

On Fig. 13 the position of contact points on a wheel and rail depending on lateral displacement of wheelset are shown. Fig. 13(a) corresponds to the Initial wheel profile; Fig. 13(b) corresponds to the Optimized profile. Comparing these plots one can see the improvement of the contact of the Optimized profile and R160 rail. Big jump of the contact point on the tread of Initial profile was splitted into two smaller jumps for Optimized profile. The more smooth transition from a tread part of wheel on a flange will decrease flange wear. The smoothly increasing concity on the flange side improves passing sharp curves. The concity of the tread of the Optimized profile is lower than concity of the Initial profile, so it is difficult to say if the Optimized profile has the same (or better) dynamic properties on the

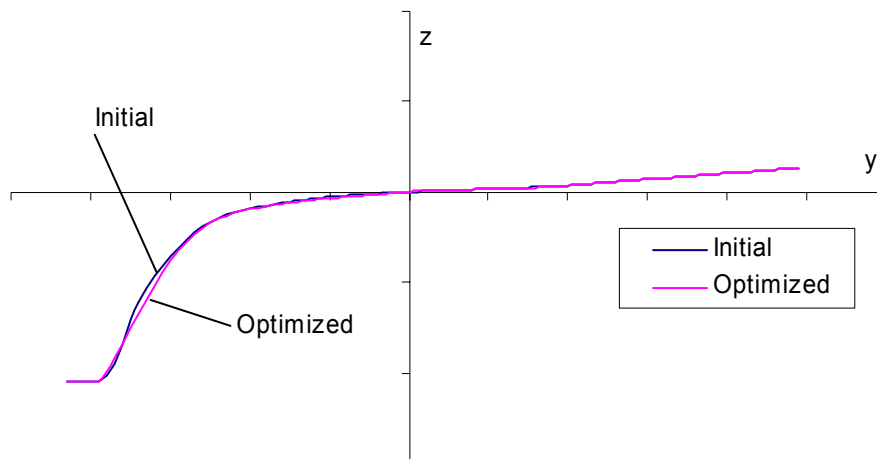


Fig. 12. Initial and optimized wheel profiles (Case - design)

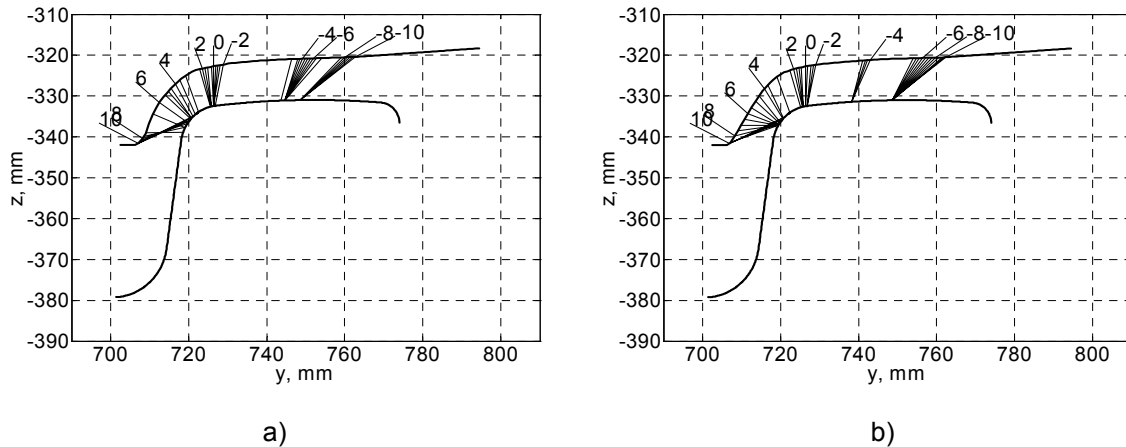


Fig. 13. Position of contact points on wheel and rail depending on lateral displacement of wheelset (Case - design)

straight track as compared to the Initial profile. The presence of small jumps of a contact point for the Optimized profile is typical for the unworn rail profile. The rail profile consists of the connected circles with different radius. As a result, when the wheel moves on the rail it misses some points on a rail and this results in jumps of contact point on a wheel and rail.

Analysing Fig. 13 one can see that for zero lateral displacement of wheelset, the wheel contact rail almost on flange root. This is different from the typical situation for railways, where for zero lateral displacement the contact point situated on the rail top and wheel tread.

The dynamic behaviour of the tramcar on Optimized wheels has been simulated with the same conditions on the curved track with the radius 150 m. The lateral displacements of first wheelset versus time presented on Fig. 14. At this time oscillations of wheelset have damped relatively fast. The Optimized wheel also has slightly less wear than the Initial one (see Fig. 15). The mean wear numbers for the left and right wheels of the first wheelset calculated for different wheel profiles are presented on Fig. 16. Light filled columns show results for Initial profile and dark filled columns correspond to the Optimized wheel profile. The decrease of wear is about 3-5% that on the year basis gives 1-2 extra weeks of wheelset exploitation. One can see that reasonable increasing of rolling radii difference gives improvement for passing curves and decreases wear rate.

Modifying a '  $y - \Delta r$  ' curve for different conditions of rolling stock and/or track and finding the corresponding wheel profile, can reduce the number of time-consuming manual selection of an optimal wheel profile.

In application of wheel design for trains the target '  $y - \Delta r$  ' curve should be different as concerned to the railways since the running speed is higher (critical speed is more important) and curves are not that sharp.

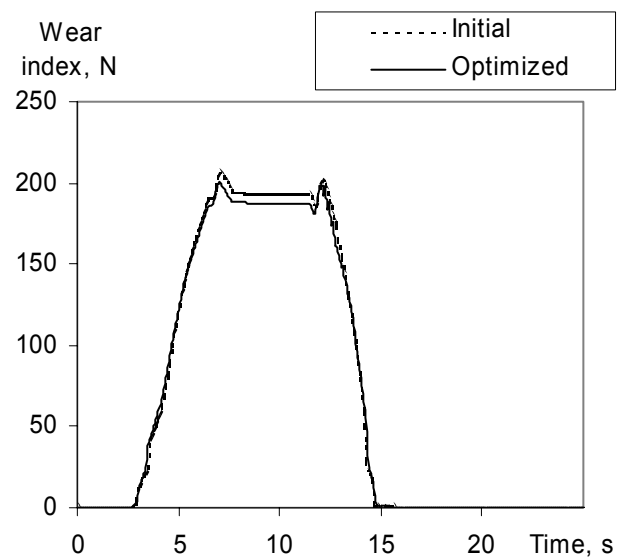
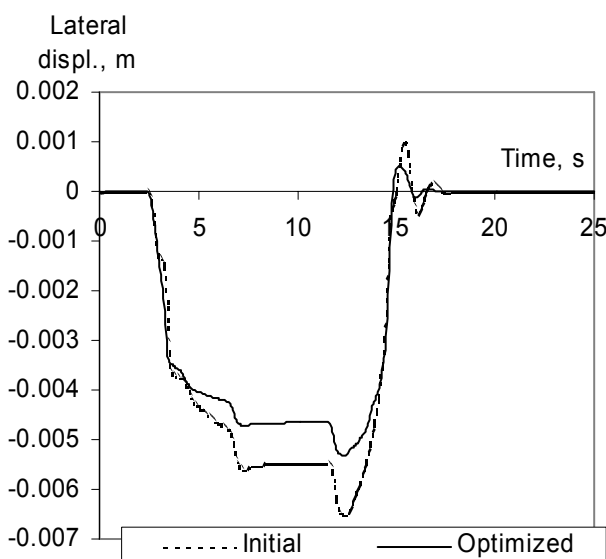


Fig 14. Lateral displacements of front wheelset vs. time

Fig 15. Wear index of the left front wheel vs. time

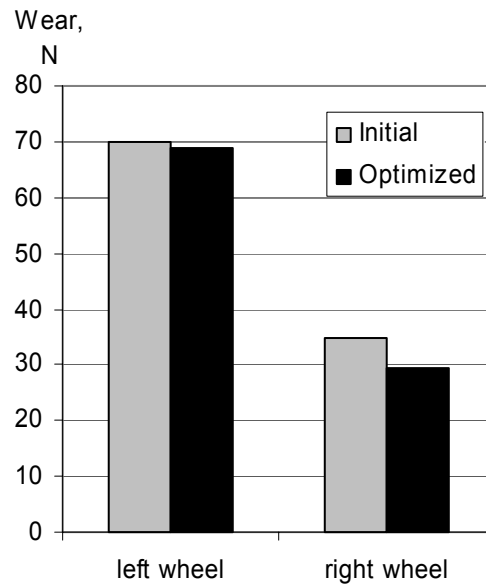


Fig. 16. The mean wear number for first wheelset

(Case - design)

(Case - design)

## 7. Conclusions

The paper presents a procedure for design of wheel profile based on the rolling radii difference function. The wheel profile with in advance defined geometrical contact properties has been obtained using numerical optimization technique.

Using this procedure a new tram wheel profile has been obtained. It has been shown that the obtained wheel profile can reduce wheel/rail wear without deterioration of dynamic performance which has been analysed using ADAMS/Rail computational package.

The procedure can also be applied to design of wheels for new rails. Using ‘ $y-\Delta r$ ’ curve (taken e.g. from the previous successful wheel/rail pair) in the wheel profile design then guaranties that the wheelset with obtained wheel profile on the new rails will have the dynamic characteristics similar to ones of the previous wheel/rail pair.

In future this procedure will be applied for design of rail profile to determining the amount of grinding. The minimization of contact stresses is also should be taken into account

Only wheel profile modification cannot solve all problems with wear and instability of vehicles. Engineers should keep in mind all factors influencing the vehicle dynamic, wear factors, maintenance costs etc. To solve such complex problems optimization methods should be widely used.

## 8. Acknowledgments

The authors would like to thank HTM (The Hague tram company) for providing measured wheel and rail profiles and tram model data. Profiles of wheel and rails were measured using MINIPROF measuring devices, manufactured by Greenwood Engineering (Denmark), whose help is greatly appreciated.

## 9. References

1. R.V. Dukkipati, Vehicle Dynamics, Boca Raton, CRC Press, ISBN 0-8493-0976-X, 2000
2. C. Esveld, Modern Railway Track, (Second Edition), MRT-Productions, Zaltbommel, ISBN 90-8004-324-3-3, 2001
3. A.H. Wickens, The Dynamic Stability of Railway Vehicle Wheelsets and Bogies Having Profiled Wheels, International Journal of Solids Structures, vol. 1, pp 319-341, 1965

4. N.K. Cooperrider, E. H. Law, et al., Analytical and Experimental Determination of Nonlinear Wheel/Rail Constraints, Proceedings ASME Symposium on Railroad Equipment Dynamics, 1976
5. A.D. de Pater, The Geometrical Contact Between Track and Wheelset, Vehicle System Dynamics, vol. 17, pp 127-140, 1988
6. V.L. Markine, Optimization of the Dynamic Behaviour of Mechanical Systems, PhD Thesis, TU Delft, Shaker Publishing BV, ISBN 90-423-0069-8, 1999
7. V.V. Toropov, Simulation Approach to Structural Optimization, Structural Optimization, vol. 1, pp 37-46, 1989
8. J.-F.M. Barthelemy, R.T. Haftka, Approximation Concept for Optimum Structural Design – a Review, Structural Optimization, vol. 5, p 129-144, 1993
9. V.V. Toropov, V.L. Markine, The Use of Simplified Numerical Models as Mid-Range Approximations, Proceedings of the 6-th AIAA/USAF/NASA/ISSMO Symposium on Multidisciplinary Analysis and Optimization, Part 2, Bellevue WA, September 4-6, ISBN 1-56347-218-X, pp 952-958, 1996
10. V.V. Toropov, F. van Keulen, V.L. Markine, L.F. Alvarez, Multipoint Approximations Based on Response Surface Fitting: a Summary of Recent Developments. In V.V. Toropov (Ed.) Proceedings of the 1st ASMO UK/ISSMO Conference on Engineering Design Optimization, Ilkley, West Yorkshire, UK, July 8-9, ISBN 0-86176-650-4, pp 371-381, 1999
11. J.J. Kalker, Three-Dimensional Elastic Bodies in Rolling Contact, Kluwer Academic Publishers, Dordrecht, ISBN 0-7923-0712-7, 1990
12. I.Y. Shevtsov, V.L. Markine, C. Esveld, Railway wheel profile optimization based on geometric wheel/rail contact, Proceedings of the 8th mini conference on Vehicle System Dynamics, Identification and Anomalies, Budapest, Hungary, 11-13 November, 2002 (to be published)